HHS Public Access

Author manuscript

Ultrastruct Pathol. Author manuscript; available in PMC 2015 July 01.

Published in final edited form as:

Ultrastruct Pathol. 2015 April ; 39(2): 153–158. doi:10.3109/01913123.2014.960542.

Electron microscopy remains the gold standard for the diagnosis of epithelial malignant mesothelioma: A case study

Elizabeth A. Oczypok, B.S. and **Tim D. Oury, M.D., Ph.D.**

Department of Pathology, University of Pittsburgh School of Medicine, 3550 Terrace Street, Pittsburgh, PA 15261

Abstract

This is a case of idiopathic epithelial malignant mesothelioma in a 47-year-old mechanic. The advent of a large battery of immunochemical markers has provided new tools for the diagnosis of mesothelioma in recent years, however, immunostaining can often be misleading or inconsistent, as demonstrated in the current case. This report highlights the lasting utility of electron microscopy in the diagnosis of mesothelioma. Ultrastructural features of epithelial mesothelioma were discernable using electron microscopy even on somewhat poorly preserved chest wall biopsy specimens from paraffin blocks. These images, combined with immunostains and a fiber analysis from the lungs, allowed for a final diagnosis of a non-asbestos related malignant epithelial mesothelioma in this patient.

Keywords

Epithelial malignant mesothelioma; electron microscopy; tremolite cleavage fragment; renal cell carcinoma

INTRODUCTION

While diagnosis of mesothelioma has become much easier in recent years with the advent of new immunochemical markers, several cases still remain challenging. In these cases, electron microscopy, which remains the gold standard for diagnosis of an epithelial mesothelioma, is still very useful. Prior to death, this patient was diagnosed with an epithelial mesothelioma based on retroperitoneal lymph node and liver nodule biopsies. Notably, immunohistochemical analysis of autopsy tissue was not typical of a mesothelioma, and gross findings at the time of autopsy were even suggestive of a metastatic renal cell carcinoma. In this case, electron microscopy was successfully used to identify ultrastructural changes that were diagnostic of an epithelial mesothelioma, even in poorly preserved tissue specimens. This case highlights the importance of electron

Corresponding Author: Tim Oury, M.D., Ph.D., tdoury@pitt.edu, S785 Scaife Hall, 3550 Terrace Street, Pittsburgh, PA 15261, 412-648-9659.

Conflict of Interest: T.D.O. serves as a consultant on medical-legal cases involving asbestos associated diseases.

Funding Disclosures: EAO is funded by the Angiopathy Training Grant (T32 HL094295).

microscopy in diagnostic pathology, especially in the face of questionable immunostaining results.

MATERIALS AND METHODS

Patient History and Hospital Course

This patient was a 47-year-old Caucasian male with no prior medical conditions who presented to the emergency department complaining of pain in his upper left extremity and neck, severe abdominal pain, and constipation. The patient had been experiencing abdominal pain for about one month prior to his hospital admission and had recently been diagnosed with chronic cholecystitis. Notably, the patient had had an abdominal ultrasound and chest x-ray carried out one month prior to being admitted to the hospital because of worsening right upper quadrant pain. At that time, the liver was reported to be normal with mild fatty infiltrates. The right kidney was normal in size. The left kidney was not evaluated at this time. The gallbladder was normal. There were no pulmonary effusions or infiltrates noted on chest x-ray. The patient had worked as a mechanic for over thirty years, including work on brakes. He had a remote smoking history.

Upon evaluation at the hospital, the patient was discovered to be in acute renal failure with a BUN of 50 and a creatinine of 4.8. He was hypertensive and, soon after admission, began to feel short of breath. Doppler ultrasound revealed thrombi in his left internal jugular, subclavian, axillary, and basilic veins. A chest x-ray revealed bilateral pleural effusions. A CT showed diffuse lymphadenopathy throughout the chest, abdomen, and pelvis. Multiple small, noncalcified lung nodules were noted within the right upper lobe and the left lower lobe. Additionally, the patient had pancreatitis, bilateral Grade I–II hydronephrosis, and a distended bladder. A radionuclide renal scan and flow study was completed four days after admission. It revealed an enlarged left kidney and normal right kidney, suggestive of obstruction or renal vein thrombosis on the left.

A PET CT done five days after admission revealed widespread metastatic disease in the liver, skeleton, and lymph nodes. There was a large uptake of tracer in the epigastrium near the head of the pancreas. The PET scan did not reveal any definitive primary lesion in the lung, but bilateral pleural effusions with some uptake of tracer were noted.

A left retroperitoneal lymph node was biopsied and showed a metastatic, poorly differentiated, epithelial neoplasm that was positive for cytokeratin, but negative for all other markers evaluated (Table 1). To further characterize the neoplasm and its site of origin, a hepatic nodule from the right lobe was biopsied one week after admission. Pathology reported that the lesion was metastatic, poorly differentiated mesothelioma. Immunohistochemistry showed that the tumor was positive for both calretinin and vimentin; it was negative for the other markers evaluated (Table 1). On the same day, the patient had a thoracentesis with removal of 1300 cc of amber-colored exudate. Cytology from the lung fluid showed large, poorly differentiated cells, consistent with a malignant epithelial neoplasm.

Eleven days after admission, the patient underwent a right thoracoscopy with a chest wall biopsy, pleural peel, and talc pleurodesis. The chest wall biopsy and pleural peel were analyzed by pathology and, although no immunochemical or other studies were performed, the final diagnosis was epithelial mesothelioma based on previous studies from the liver biopsy.

The patient's condition quickly deteriorated. He was transferred to hospice care where he died from his metastatic disease just three weeks after his initial admission to the hospital.

Post-mortem examination

An autopsy was conducted about two days after death. Cancerous tissue was found in the right pleural space, retroperitoneum, lungs, mediastinum, para-aortic lymph nodes, right ventricle of the heart, liver, and small intestine. A 3 × 2 × 2 cm tumor was also identified in the upper pole of the right kidney. The right chest cavity was filled with fibrous adhesions. No adhesions were noted in the left chest cavity, but there were about 2000 cc of bloody exudate in the left pleural cavity. No pleural plaques were seen. The autopsy indicated that the right lung was surrounded by a 0.2–0.5 cm firm, fibrous rind. This finding is consistent with tumor and/or the patient's recent talc pleurodesis. The left lung contained small subpleural nodules in both the upper and lower lobes as well as a 2.5 × 2 × 2 cm infarct in the lower lobe. Firm, matted lymph nodes were diffusely prominent in the chest and abdomen, especially in the para-aortic region. Microscopic analysis of the tumor tissue from various organs was hindered by autolytic changes, but a metastatic epithelioid neoplasm with clear to eosinophilic cytoplasm was still identifiable on histological sections.

Electron microscopy

Tumor was removed from the paraffin block of the pre-mortem right chest wall surgical specimen. The tissue was deparaffinized in xylenes, rehydrated, placed in 0.1 M cacodylate buffer, embedded in epoxy-resin, and mounted on an electron microscopy stud for sectioning and analysis by transmission electron microscopy (TEM).

Tissue Digestion and Fiber Analysis

A 0.542 g autopsy specimen consisting of normal tumor-free lung tissue from the left upper and lower lobes was digested using the sodium hypochlorite method as described previously [1]. For analysis, the residue was divided between two 0.45 μm Millipore filters, one for asbestos body quantification by light microscopy and another for fiber analysis by scanning electron microscopy (SEM) and energy dispersive x-ray analysis (EDXA).

RESULTS

Histological Examination

This case was originally presented to the authors as part of a medical-legal consultation, and, as such, several consulting pathologists were involved in analysis of the tissue specimens. Hematoxylin and eosin (H&E) staining was carried out on biopsy tissue obtained prior to death from the right chest wall and shows enlarged, vesicular nuclei with prominent nucleoli

and moderately abundant clear to eosinophilic cytoplasm (Figure 1a). These results were suggestive of an epithelioid metastatic tumor.

An extensive immunohistochemical analysis was carried out on both the surgical biopsy and autopsy specimens (Table 1). The variability among the numerous immunostains demonstrates the complicated nature of the case and again highlights the usefulness of electron microscopy for diagnosis. An outside consulting pathologist performed several immunochemical stains on tissue from the pre-mortem right chest wall biopsy and the results are summarized in Table 1. This pathologist also completed a large panel of immunostains on lung tumor samples from the autopsy. The institution where the autopsy was carried out completed their own panel of immunostains on the left pararenal mass and mesenteric mass. The slides were obtained and the results were re-interpreted by the authors of this paper (T.D.O.). Autopsy tissue blocks of the left pararenal mass, right kidney, and matted lymph nodes were used for a separate panel of immunostains that were carried out and interpreted by the authors (T.D.O.). Tumor tissue from the right kidney was also examined after H&E staining. This showed large cells with clear cytoplasm, resembling a renal cell carcinoma (Figure 1B). A final analysis was completed by the authors on pre-mortem chest wall biopsy material.

The combination of various immunostains on tissue from both surgical biopsies and the autopsy were not typical of mesothelioma. Furthermore, the discovery of a renal tumor at the time of the autopsy, as well as the presence of clear cells with enlarged nuclei on histological analysis of multiple tumor tissue samples, suggested a possible diagnosis of renal cell carcinoma. Therefore, a definitive diagnosis could not be made from histology and immunochemistry alone. Thus, the gold standard of electron microscopy was carried out on the chest wall biopsy tissue to further evaluate the tumor for ultrastructural features of epithelial mesothelioma.

Electron Microscopy

Electron microscopy was carried out on tissue from the right chest wall biopsy specimen that had been surgically removed before the patient's death (Figure 1C and 1D). Normally, electron microscopy is best done on tissue that is appropriately fixed at the time of removal from the body. Here, the tissue had been paraffin-embedded prior to sectioning and thus, the cellular architecture was poorly preserved. However, electron microscopy did reveal several areas with numerous elongated microvilli and enlarged desmosomes. There were perinuclear tonofilaments present in some areas as well. These discernable ultrastructural features are most consistent with the diagnosis of an epithelioid type malignant mesothelioma [2].

Tissue Digestion and Fiber Analysis

A scan of the entire first filter at 200X by light microscopy revealed one definitive and a second possible asbestos body, indicating that between two and six asbestos bodies were present per gram of tissue-wet weight after correcting for paraffin embedding [1]. This is below the value normally seen in individuals with occupational exposures to asbestos and is in the range of levels seen for non-asbestos exposed controls [1]. An area measuring 2.35 mm^2 of the second filter revealed ten uncoated fibers at least 5 μm in length and with an

aspect ratio of greater than 3:1. These included two talc fibers, two silica-only fibers, three titanium fibers, one glass fiber, and two tremolite cleavage fragments. Therefore, there are 682 tremolite cleavage fragments per gram of tissue wet weight. This value is in the range of values seen in control populations with no known asbestos exposure and is below that which is seen in individuals with known occupational asbestos exposure [1].

DISCUSSION AND FINAL DIAGNOSIS

In summary, this was a 47-year-old truck mechanic with no prior medical problems who developed an aggressive malignant mesothelioma not attributable to asbestos exposure and best classified as an idiopathic mesothelioma with metastases to the abdominal organs, kidney, heart, and lymph nodes. Mesothelioma can be difficult to distinguish from metastatic renal cell carcinoma (RCC), as both cancers are positive for keratin and vimentin. Additionally, high amounts of cytoplasmic glycogen can give both cell types a clear appearance. This, combined with enlarged nuclei and nucleoli in both types of malignant cells, makes mesothelioma and RCC quite similar histologically.

Classically, RCC and mesothelioma can be distinguished using various immunostains. RCC usually is PAX-8 positive and calretinin negative while most mesotheliomas are PAX-8 negative and calretinin positive. Mesotheliomas also usually stain positive for cytokeratin 5/6 and cytokeratin 7. In this case, autopsy specimens were negative for calretinin, but also negative for PAX-8 (Table 1). The kidney tissue was negative for cytokeratin 5/6 and cytokeratin 7, but the lymph nodes were focally positive for cytokeratin 5/6 and positive for cytokeratin 7. Overall, the tissue was hard to examine histologically due to extensive autolytic changes post-mortem. The surgical biopsy specimens were well-preserved and showed calretinin positivity in both the chest wall and liver nodule. PAX-8 was negative in the chest wall tissue as well, suggesting a mesothelioma. CD10 positivity is seen in 81% of RCC cases and can be a helpful diagnostic marker of RCC as well [3]. However, about half of all epithelial mesotheliomas also express CD10 [3]. Here, autopsy specimens revealed variable CD10 expression, while CD10 was negative in the liver nodule biopsy (Table 1). This variability further stresses the difficulty of differentiating various types of cancer using immunostaining alone.

In order to diagnosis this cancer, electron microscopy was carried out on tissue sections that were taken from paraffin-embedded chest wall biopsy blocks. While not ideal, enough ultrastructural features were present to identify this malignancy as an epithelioid mesothelioma and not a renal cell carcinoma. Perinuclear tonofilaments, enlarged desmosomes, and elongated microvilli, all distinguishing markers of mesothelioma, were observed [2]. Notably, while our samples clearly showed abundant, elongated microvilli, the lack of microvilli cannot be used to rule out mesothelioma, as some mesothelioma cells may possess only a few short microvilli [4]. Microvilli ultrastructural features such as a lack of core filaments and rootlets and minimal glycocalyx may also be used to further identify mesothelial microvilli from those found on other forms of cancer [5].

Finally, as the majority of mesotheliomas are caused by asbestos, the patient’s asbestos exposure was carefully examined to determine if the mesothelioma was asbestos-related.

First, the patient had labored for thirty years as a truck mechanic where he worked with asbestos-containing brake linings and other materials. These products contain chrysotile asbestos, which is less pathogenic than amphiboles. Furthermore, several epidemiological studies have shown that there is no increased occupational risk of mesothelioma in mechanics and other automobile workers who are regularly exposed to these products [6–13]. Indeed, in the current case, SEM analysis of lung tissue revealed no evidence of elevated asbestos fibers compared to control individuals with no history of asbestos exposure. Only tremolite cleavage fragments, which are non-asbestiform, were seen. These fragments have the same chemical composition of asbestiform tremolite fibers, but are not crystallized in the same way [14]. Tremolite cleavage fragments are shorter in length and are thicker (usually greater than 1 μm diameter) than asbestiform tremolite, which is usually long and slender (less than 1 μm in diameter) [14,15]. These structural differences affect the pathogenicity of the fiber, and there is no evidence that tremolite cleavage fragments contribute to the pathogenesis of mesothelioma [16,17]. Therefore, there is no evidence that this patient's malignant mesothelioma is due to occupational asbestos exposure. These results are consistent with previous studies demonstrating no increased risk of mesothelioma in mechanics and no evidence of elevated levels of asbestos in the lungs of these workers [6–13].

References

1. Roggli, VL.; Sharma, A. Analysis of Tissue Mineral Fiber Content. In: Roggli, VL.; Oury, TD.; Sporn, TA., editors. Pathology of Asbestos-Associated Diseases. 2. New York: Springer-Verlag; 2004. p. 309-354.
2. Oury TD, Hammar SP, Roggli VL. Ultrastructural features of diffuse malignant mesotheliomas. Hum Pathol. 1998; 29:1382–1392.10.1016/S0046-8177(98)90006-5 [PubMed: 9865823]
3. Ordóñez NG. The diagnostic utility of immunohistochemistry in distinguishing between mesothelioma and renal cell carcinoma: a comparative study. Hum Pathol. 2004; 35:697–710.10.1016/j.humpath.2003.11.013 [PubMed: 15188136]
4. Dardick I, Jabi M, McCaughey WT, et al. Diffuse epithelial mesothelioma: a review of the ultrastructural spectrum. Ultrastruct Pathol. 1987; 11:503–533. [PubMed: 3318058]
5. Fresco, R. Malignant Mesothelioma Electron Microscopy. In: Pass, HI.; Vogelzang, N.; Carbone, M., editors. Malignant Mesothelioma: Pathogenesis, Diagnosis, and Translational Therapies. 1. New York: Springer; 2005. p. 508-516.
6. Wong O. Malignant mesothelioma and asbestos exposure among auto mechanics: appraisal of scientific evidence. Regul Toxicol Pharmacol. 2001; 34:170–177.10.1006/rtph.2001.1491 [PubMed: 11603959]
7. Goodman M, Teta MJ, Hessel PA, et al. Mesothelioma and lung cancer among motor vehicle mechanics: a meta-analysis. Ann Occup Hyg. 2004; 48:309–326.10.1093/annhyg/meh022 [PubMed: 15148053]
8. Butnor KJ, Sporn TA, Roggli VL. Exposure to brake dust and malignant mesothelioma: a study of 10 cases with mineral fiber analyses. Ann Occup Hyg. 2003; 47:325–330.10.1093/annhyg/meg048 [PubMed: 12765873]
9. Marsh GM, Youk AO, Roggli VL. Asbestos fiber concentrations in the lungs of brake repair workers: commercial amphiboles levels are predictive of chrysotile levels. Inhal Toxicol. 2011; 23:681–688.10.3109/08958378.2011.580472 [PubMed: 21671853]
10. Laden F, Stampfer MJ, Walker AM. Lung cancer and mesothelioma among male automobile mechanics: a review. Rev Environ Health. 2004; 19:39–61. [PubMed: 15186039]

11. Hessel PA, Teta MJ, Goodman M, Lau E. Mesothelioma among brake mechanics: an expanded analysis of a case-control study. Risk Anal. 2004; 24:547–52.10.1111/j.0272-4332.2004.00458.x [PubMed: 15209929]
12. Rake C, Gilham C, Hatch J, Darnton A, Hodgson J, Peto J. Occupational, domestic and environmental mesothelioma risks in the British population: a case-control study. Br J Cancer. 2009; 100:1175–83.10.1038/sj.bjc.6604879 [PubMed: 19259084]
13. Finley BL, Pierce JS, Paustenbach DJ, Scott LL, Lievense L, Scott PK, Galbraith DA. Malignant pleural mesothelioma in US automotive mechanics: Reported vs. expected number of cases from 1975 to 2007. Regul Toxicol Pharmacol. 2012; 64:104–116.10.1016/j.yrtph.2012.05.015 [PubMed: 22668748]
14. Occupational Exposure to Asbestos, Tremolite, Anthophyllite and Actinolite, Section IV-Mineralogical Considerations (57 FR 24310). Occupational Health and Safety Administration (OSHA), U.S. Department of Labor; Released June 1992https://http://www.osha.gov/pls/oshaweb/owadisp.show_document?p_table=PREAMBLES&p_id=785 [Accessed 7 April 2014]
15. Harper M, Lee EG, Doorn SS, Hammond O. Differentiating Non-Asbestiform Amphibole and Amphibole Asbestos by Size Characteristics. J Occup Environ Hyg. 2008; 5:761–770.10.1080/15459620802462290 [PubMed: 18828048]
16. Addison J, McConnell EE. A review of the carcinogenicity studies of asbestos and non-asbestos tremolite and other amphiboles. Regul Toxicol Pharmacol. 2008; 52:S187–199.10.1016/j.yrtph.2007.10.001 [PubMed: 18006199]
17. Gamble JF, Gibbs GW. An evaluation of the risks of lung cancer and mesothelioma from exposure to amphibole cleavage fragments. Regul Toxicol Pharmacol. 2008; 52:S154–186.10.1016/j.yrtph.2007.09.020 [PubMed: 18396365]

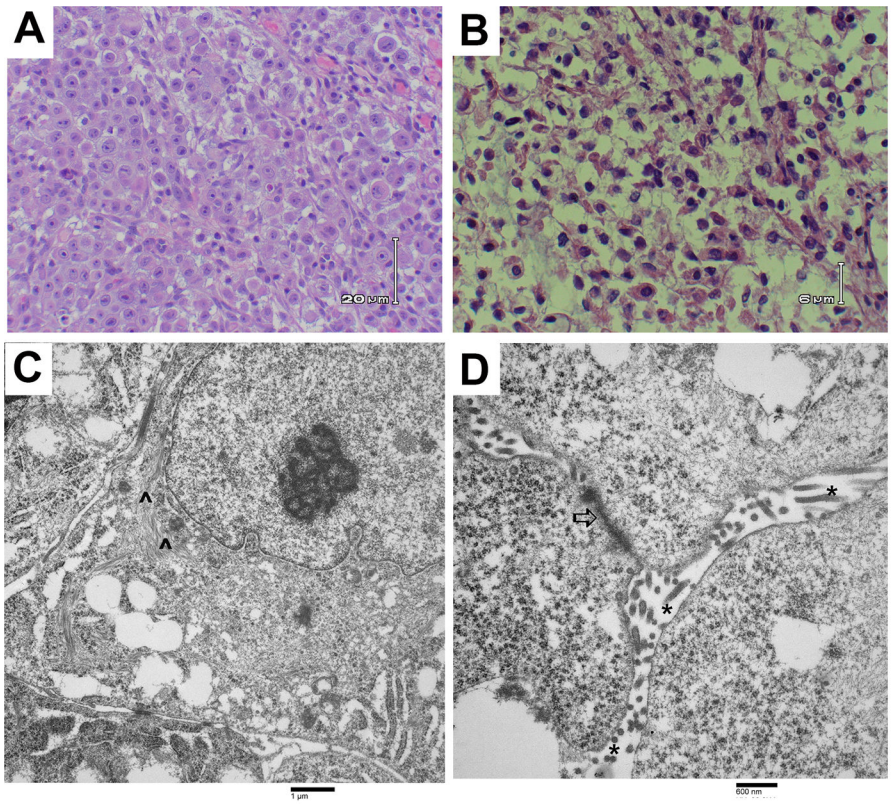

Figure 1. Images of malignant mesothelioma from patient tissue samples

(A) Light microscopic image of H&E-stained right chest wall biopsy material showing large cells with clear to eosinophilic cytoplasm and enlarged nuclei with prominent nucleoli, typical of an epithelial mesothelioma. (B) Light microscopic image of H&E-stained right kidney tumor tissue from the autopsy. Cells are large with clear cytoplasm, suggestive of a renal cell carcinoma or a malignant mesothelioma. (C and D) Transmission electron photomicrographs of the right chest wall biopsy showing ultrastructural features of mesothelioma including perinuclear tonofilaments (^), fragmented, elongated microvilli (*), and giant desmosomes (⇧).

Table 1

Immunochemical staining of patient biopsy and autopsy tissue samples

	BIOPSY SPECIMENS				AUTOPSY SPECIMENS						
Immunostain	**Retroperitoneal Lymph Node***	**Liver Nodule***	**Right Chest Wall$^{\Psi}$**	**Right Chest Wall**	**Lung Specimen 1$^{\Psi}$**	**Lung Specimen 2$^{\Psi}$**	**Mesenteric Mass$^{\#}$**	**Left Pararenal Mass$^{\#}$**	**Left Pararenal Mass**	**Right Kidney**	**Matted Lymph Nodes**
BCL-2		−									
Ber-EP4			+, membrane	+, membrane	+, membrane		+, membrane	+, membrane			
CA19-9		−									
Calretinin		+, nucleus	+, nucleus	+, nucleus	focal +	+, nucleus	focal +	−	−	−	−
CD10		−							+/−	+/−	+/−
CD15		−									
CEA	−				−		focal +	+			
CK20	−				−						
CK5/6			weak +	−	−	+			−	−	focal +
CK7	−				−				−	−	+
D2-40			−	−	−						
Pan-ker	+				+				+	+	+
PAX-8			+, nucleus	−	−	+, nucleus			−	−	−
PLAP	−										
PSA	−										
RCC				−					−	−	−
TTF-1		−	−		−						
Vimentin		+		+							
WT-1			−		−				+	−	−

*Immunostains were carried out in original diagnosing hospital and interpreted in the pathology report. Slides were not obtained for re-interpretation.

#Immunostains were done during the original autopsy. The slides were obtained and re-interpreted by the author (T.D.O.).

ΨImmunostains were carried out by an outside consulting pathologist and re-interpreted by the author (T.D.O.).

For all other samples, new sections were cut from existing tissue and immunostained by the authors. Results were interpreted by the author (T.D.O.).